

Contents

<u>Contents</u>	1
<u>Introduction</u>	2
<u>Purpose and Current Development of UAV's</u>	3
The First Operational UAV's : Drones	3
VTOL UAV's	4
Ducted Fan UAV's	5
<u>Planning Propulsion System Optimisation</u>	7
<u>Modifying Existing Fan Units</u>	8
<u>Introduction</u>	8
<u>Previous Attachment Method</u>	9
<u>Modifications to Adaptor Attachment</u>	9
<u>Modifications to Fan Attachment</u>	10
<u>Analytical Ducted Fan Optimisation</u>	11
<u>Blade Element Theory</u>	12
Theory	12
Comparison with Test Results	14
Determining Optimum Fan Design	14
<u>Momentum Theory</u>	16
<u>Displacement Theory</u>	17
<u>Design Approximations</u>	19
<u>Conclusion to Fan Analysis</u>	20
<u>Fan Detail Design</u>	21
<u>Calculation of Blade Angles</u>	21
<u>Initial Stress Analysis</u>	22
<u>3D CAD Modelling</u>	23
<u>Computational Fluid Dynamics (CFD) Analysis</u>	25
Boundary Conditions and Set-up	25
Results	26
Conclusion	26
<u>Fan Manufacture</u>	26
<u>Conclusion</u>	27
<u>References</u>	28

Introduction

This report details work carried out as part of the 'Flying Platform' project at the University of Exeter. This is an ongoing project attempting to develop an autonomous flying vehicle. A detailed explanation of the purpose of this type of vehicle is included as a subsection of this introduction. It is hoped that by explaining in detail the purpose the functional requirements will become clear.

Specifically work relating the ducted fan units is covered in this report. These units provide thrust for both lift and control purposes. Figure 1 shows the basic layout of the platform, a large number of components are omitted from this diagram. It can be seen that there are four small ducted fan units located at the periphery of the structure and a single larger unit located at the centre. The central unit is the primary thrust generator while the four smaller units provide some lift while also acting as stability control thrusters.

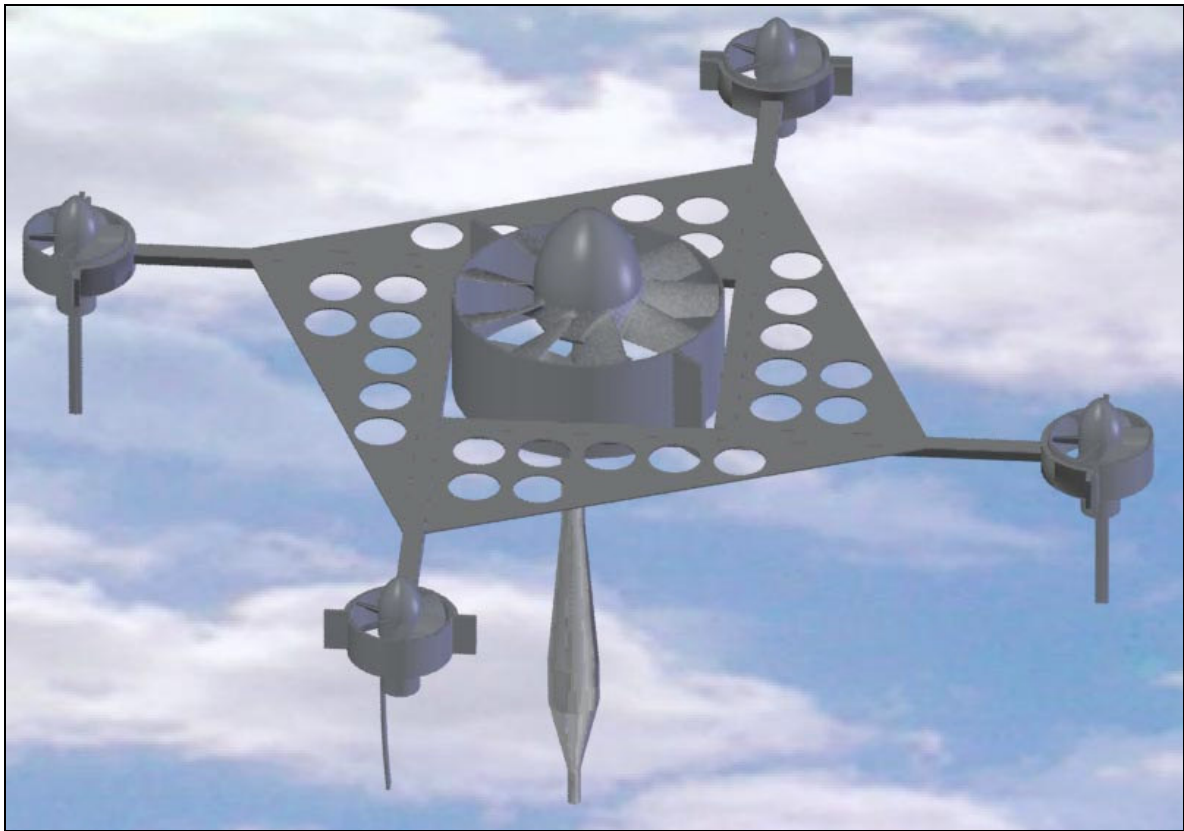


Figure 1 : Flying Platform Layout

Existing commercially available units were found to be suitable for control purposes with some minor modifications. These modifications were carried out and a full explanation of this work is detailed.

It was found that none of the commercially available units were entirely suitable for the central unit. It was decided to design an optimised unit for use the following year while continuing with the best commercial unit for this year. Work on the optimised central unit is detailed here. This has been successful in identifying the potential increase in performance, completing detailed design and identifying a suitable manufacturing route. However, due to time constraints manufacture has not been completed.

Manufacturing contacts at *Howmet Castings* are aware that the project is ongoing and are prepared to work with students in 2004-5.

Purpose and Current Development of UAV's

The First Operational UAV's : Drones

Autonomous flying vehicles more commonly known as unmanned aerial vehicles (UAV's) have a variety of uses; primarily military at the current time. 'Drones' have become an integral part of the high-tech air force as demonstrated by the United States Air Force (USAF). The *MQ1-Predator*, see Figure 2, is a sophisticated robotic military aircraft capable of surveillance and bombing missions. The *Predator* was used to assassinate al-Qaida leader, Qaed Salim Sinan al-Harethi by launching a surface to air missile in November 2002¹. The craft was able to track the targets and launch its weapons while being controlled remotely by CIA staff located in Washington! This type of strike represents the beginning of a new era in warfare since this is the first time that such a complete mission has been conducted by a remotely controlled robot.



Figure 2 : The MQ1-Predator

The benefits of using an unmanned craft for such operations are that the financial and political costs of loosing a manned aircraft are avoided and so missions that would previously have been regarded as overly risky can now be launched. Drones are the first stage in implementing the USA's Future Combat System (FCS); a 'network-centric' force built around a shared data capability². This will see heavy tanks replaced by lightweight rocket launchers able to strike targets 20 times more distant. This capability is realised since each FCS weapons launcher is actually a group of vehicles connected by a data network, including the ground based rocket launcher and both ground and air based robotic 'scouts'.

This capability will allow its possessors to conduct highly 'asymmetric warfare' against enemies of lesser technological means. This capability is becoming vital to the USA's ability to maintain a military presence in at least 36 different nations around the world³.

UAV's are operational for civilian surveillance and have been used to aid the policing of large demonstrations. The French authorities used drones to monitor the large protests around the G8 summit in Avian that took place in May 2003⁴.

There are also potentially scientific and industrial applications although there have been problems with certification. Despite this a civilian version of the *Predator*, the *Altair*, flew for the first time on the 9th June 2003⁵. It has been suggested that the *Altair* could be used to monitor dangerous situations such as volcanoes or forest fires, or conduct lengthy data collection over the oceans. The *Altair* attempts to avoid the potential dangers of unmanned flight through the use of a collision-avoidance system and a voice relay to allow air traffic controllers to talk to its ground-based pilots. It is designed to fly continuously for up to 32 hours, and reach an altitude of 16km. Assuming that the cost of such systems can be reduced drones are set to replace helicopters for many industrial applications such as power line survey.

VTOL UAV's



Figure 3⁶ : UAV on Carrier/Launcher

Despite their advantages the majority of operational UAV's have only a limited capability to operate from FCS carrier vehicles. To do this they generally require rockets or catapults for takeoff and nets or parachutes for landing. Vertical take off and landing (VTOL) capability will negate the need for such clumsy measures. Figure 3 shows the *iSTAR* UAV mounted on an autonomous carrier/launcher vehicle, the *MDARS-E*.

The ability to hover in a fixed position is closely linked with VTOL capability, while monitoring a target in surveillance missions this has obvious benefits.

UAV's with VTOL and hovering abilities are therefore an important type of UAV that serve a different function to that of existing drone aircraft. Such craft are smaller and will serve a vital role in building the USA's FCS. What the FCS requires are '*Multipurpose Security and Surveillance Mission Platforms*' (MSSMP's) forming a distributed network of remote sensors mounted on VTOL platforms. The MSSMP program began in 1992.

The intent of such systems has been described as

*"...not necessarily to provide sensing while in flight but to provide the commander with a rapidly deployable/recoverable, air-mobile, day/night, all-weather, real-time, unmanned system which will provide autonomous surveillance, detection, and assessment capabilities. These capabilities will provide timely mission-essential information on enemy activity and terrain. It will also provide commanders with an early warning device to aid them with force protection planning."*⁷



Figure 4 : Grumman's *Fire Scout*

The simplest type of VTOL UAV from a developmental point of view is the type based on the proven technology of helicopters, with the addition of a control system to allow autonomous flight. Northrop Grumman's *Fire Scout*, Figure 4, has officially been named as the Class IV unmanned aerial system (UAS) for the US Army's FCS⁸.

However, helicopter based designs are far from ideal for the UAV application. This type of vehicle may be required to fly in close proximity to obstacles or confined spaces such as narrow streets or even corridors. The exposed rotors of helicopters are extremely vulnerable in this situation.

Additionally there are numerous other examples of UAV's such as tilt rotor tactical UAV's which have completed extensive flight tests for Bell Helicopters. This type of vehicle is outside of the scope of this report, here we are interested in the MSSMP type of vehicle, specifically those that have a VTOL capability and are not based on helicopter technology with its inherent limitations discussed above and in more detail in the next section.

Ducted Fan UAV's

Ducted fan UAV's replace the large exposed rotor of helicopters with one or more smaller diameter rotors enclosed within a duct. This allows them to operate close to or even touching obstacles with a greatly reduced risk of damage, either to themselves or to other objects they may come into contact with.

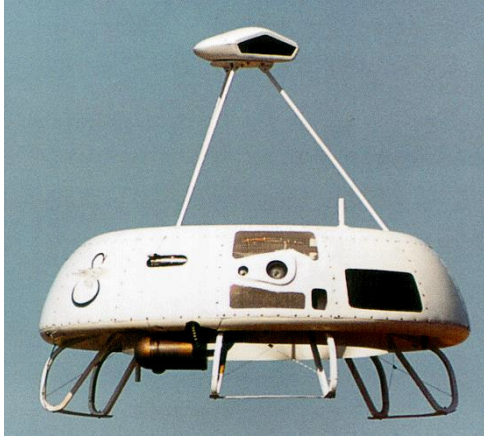


Figure 5⁹ : The Sikorsky Cypher

In January 1997 the USA demonstrated the MSSMP system by using a *Sikorsky Cypher* to fly down city streets, look through windows and continue observation after landing on the roof of a two-story building⁷. Such vehicles are expected to have widespread applications in policing¹⁰.

The *Cypher* is essentially a helicopter with the rotor enclosed within the fuselage. Although it appears unconventional the only special features are the contra-rotating rotors, as demonstrated by the *Sikorsky Advanced Blade Concept* in the 1970's, and the shrouded fantail, as demonstrated by the *S-67* and *S-76 LH Fantail Demonstrator*¹¹.

The *Cypher II* improves on the original *Cypher* through the addition of removable wings and a larger 'pusher' ducted fan. This allows dual mode flight; as both helicopter and fixed wing aircraft, greatly extending range while maintaining VTOL capability.



Figure 6¹² : Sikorsky Cypher II

The *Cypher* series of aircraft have overcome the major functional obstacles for an MSSMP. However, it remains inherently complex since it relies on the proven helicopter technology of cyclic and

collective rotor blade feathering with the additional complexity of contra-rotating rotors. Since the complexity is mechanical and not simply limited to the electronic control system the manufacturing and maintenance costs of such vehicles are unlikely to be reduced substantially and it is likely to remain difficult to construct very small versions.

There have been a number of attempts to produce designs that are far simpler in mechanical terms. As far as we are aware three solutions have been attempted. The first two methods involve using a single large ducted fan with either articulated lifting surfaces in the fan wake or pneumatic control of the fan wake by injecting compressed air¹³. The third approach is to use a number of smaller ducted fan units positioned about the centre of gravity (C of G) so that by the relative speeding up and slowing down of pairs of fans the required control moments can be generated.

The *iSTAR*, Figure 7, is a well-established single duct VTOL UAV manufactured primarily by *Allied Aerospace* with *BAe Systems* and *QinetiQ* joining the development group in 2001.¹⁴ This design uses a single fixed pitch propeller mounted inside a duct, fixed stators prevent precession due to the reaction torque on the fan while control vanes facilitate stability control and directional flight. An unusual feature of this design is that during high speed cruising the airfoil-shaped duct provides additional lift improving efficiency. The *iSTAR* completed fully autonomous flight tests, taking off, moving between waypoints and landing on target, in March 2004.¹⁵

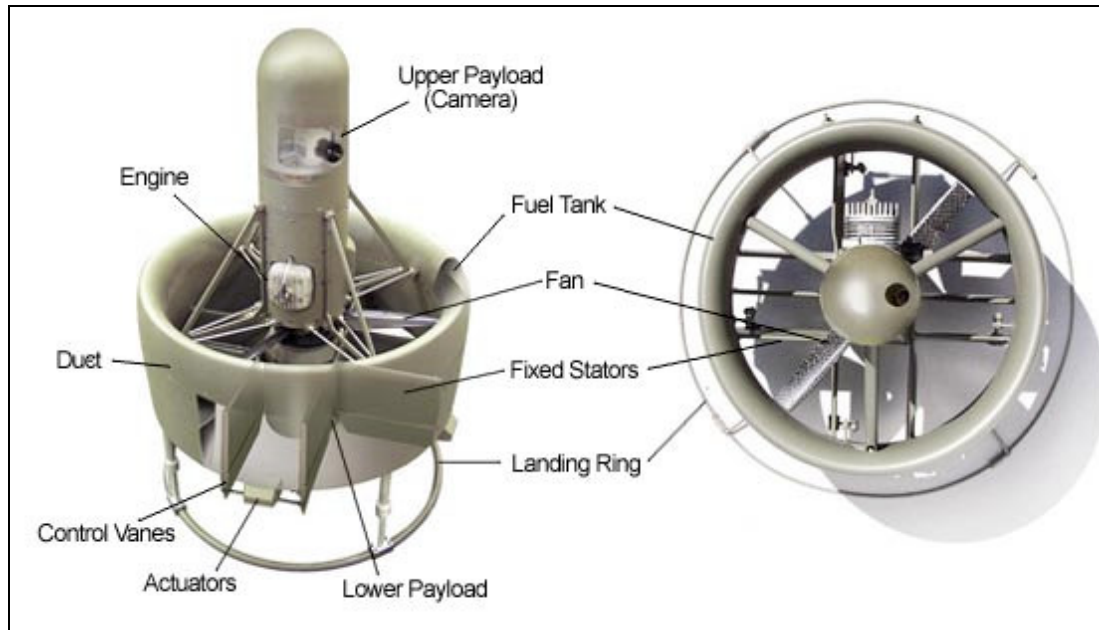
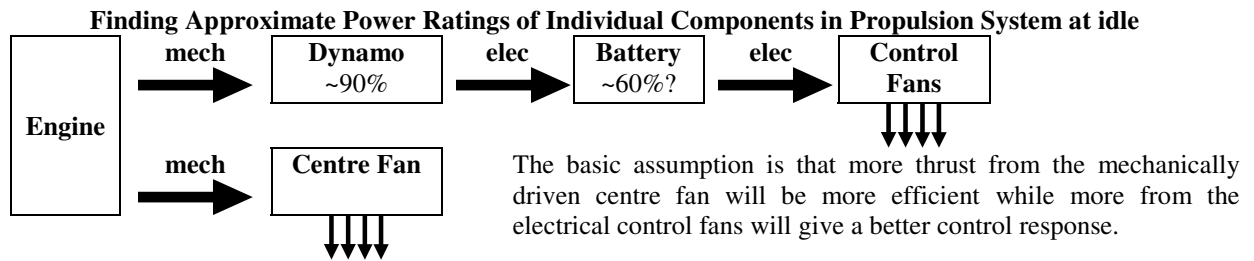


Figure 7 : Allied Aerospace ‘iSTAR’

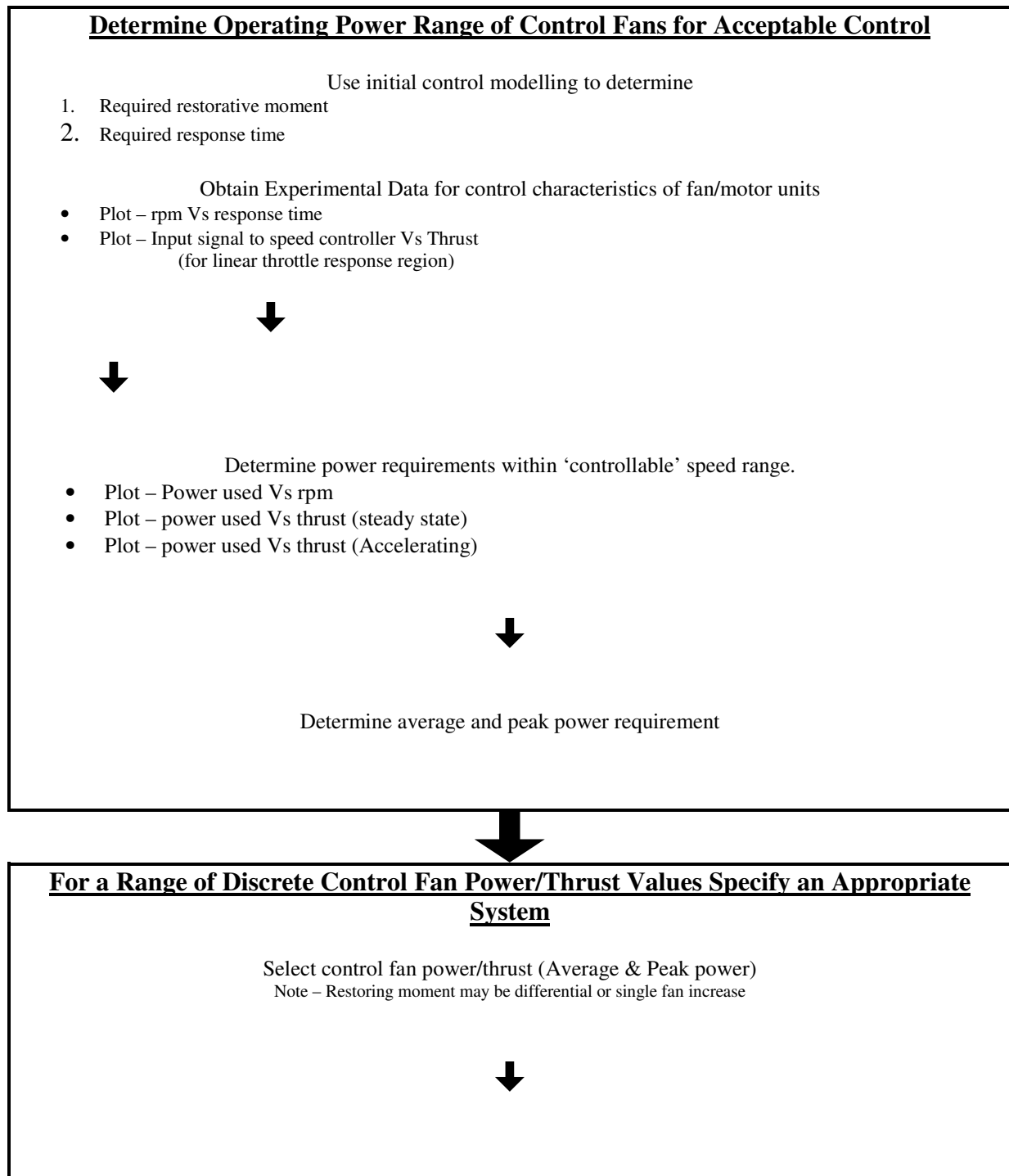
The final method, that of generating control moments by changing the thrust produced by pairs of fans, is the simplest from both control and mechanical points of view. This method is the one investigated here.

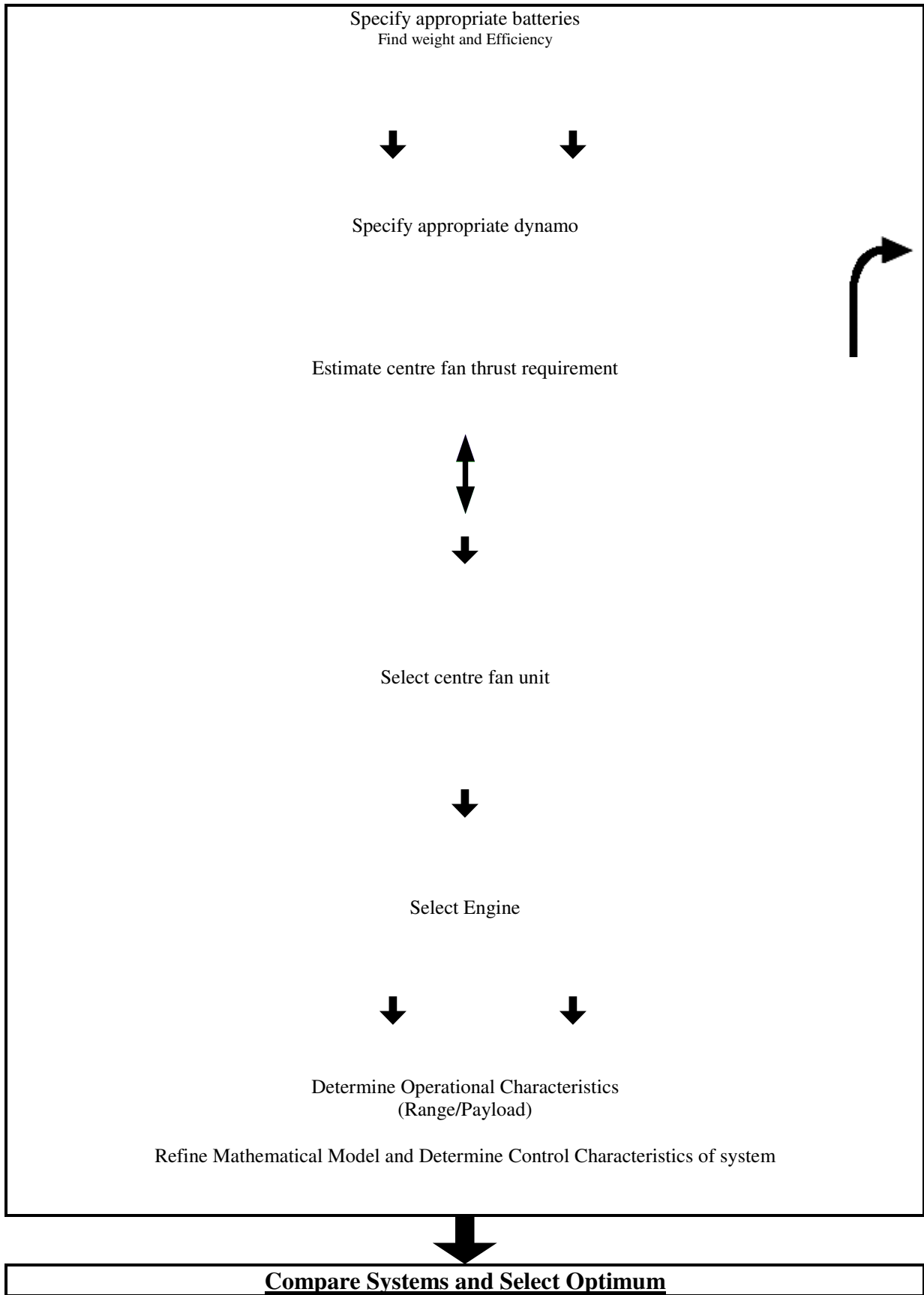
Planning Propulsion System Optimisation

The propulsion system optimisation involved complex interactions between components and iterative steps in their specification.



Flow Chart





Modifying Existing Fan Units

Introduction

The fan units used in the 2002/3 Flying Platform Project had been found to have a dangerous fault. The fans are attached to the motor spindle via an adaptor. The methods of

attachment of the adaptor to the spindle and the fan to the adaptor were both inadequate. Extreme angular deceleration is encountered in situations such as when power is suddenly cut off while the motors are running at full speed (32,000 rpm). Such deceleration had been found to cause the fans to detach from the spindle with the result that the fans would rapidly accelerate away from the platform due to the remaining angular velocity and thrust producing nature of the fans. This has potentially dangerous consequences as well as being extremely inconvenient.

Before any testing was carried out it was decided to modify the fans so as to remove this problem. After consulting with Dr Martin Jenkins and Colin Camp a simple and efficient method of achieving this was decided upon. A detailed machining procedure was drawn up to ensure the required high precision and the machining was subsequently carried out by the author.

Previous Attachment Method

The previous attachment method can be seen in Figure 8. The adaptor was pushed onto the motor spindle and secured with two grub screws. The screws pressed against the plain shaft with no real positive engagement. The fan was then fitted to the adaptor and clamped against the shoulder using a single nut.

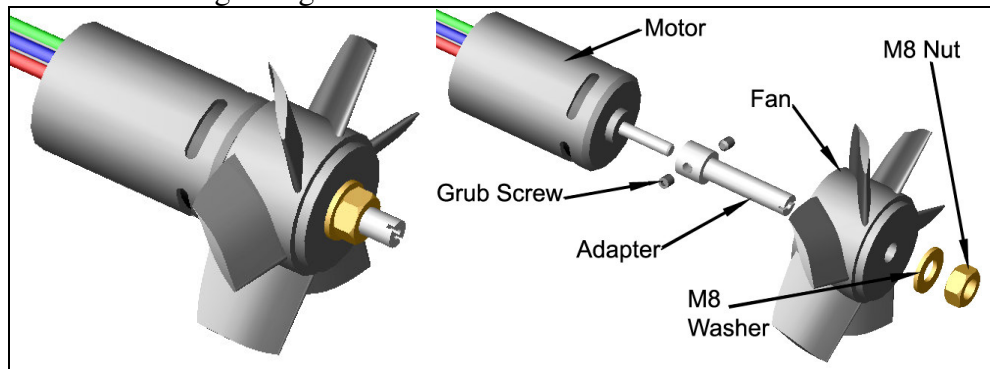


Figure 8 : Fan assembled to motor, showing previous attachment method

Modifications to Adaptor Attachment

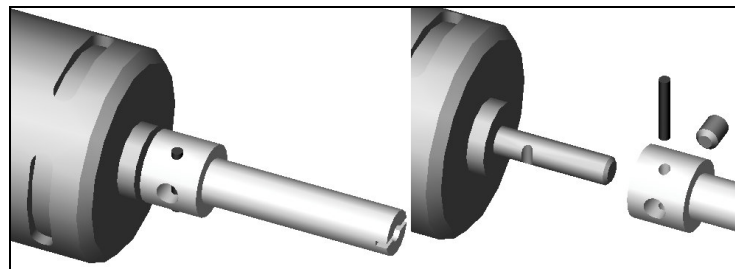


Figure 9 : Fan assembled to motor, showing modified attachment method

Modification involved drilling through both the adaptor and the motor spindle at distance of 3.77 mm from the edge of the adaptor. This put a hole in the adaptor and a semi-circular groove in the spindle. A roll pin was then inserted in order to fix the adaptor to the spindle.

Although the fitting of a pin may at first seem a trivial operation great care was required in the machining of the hole as the adaptor was aluminium while the spindle is a hardened steel. The following sequence was agreed upon.

1. 'Clock' Milling Machine (to align the vice with the axis of the machine)
2. Clamp the adaptor, fitted to the spindle, with the motor body supported by packing.

3. Zero the machine against the edge of the vice using an edge finder (this gives the precise position of the adaptor since it is in contact with the vice)
4. Move the milling head from the zero position to the precise position to be drilled.
5. Face up the collar (mill a small flat)
6. Centre drill
7. Drill through both the adaptor and the spindle in one operation. Great care being taken as the drill hits the hardened steel with a tendency to pull through the aluminium.
8. Finish the hole using a tapered ream
9. Fit a pin into the hole.

Modifications to Fan Attachment

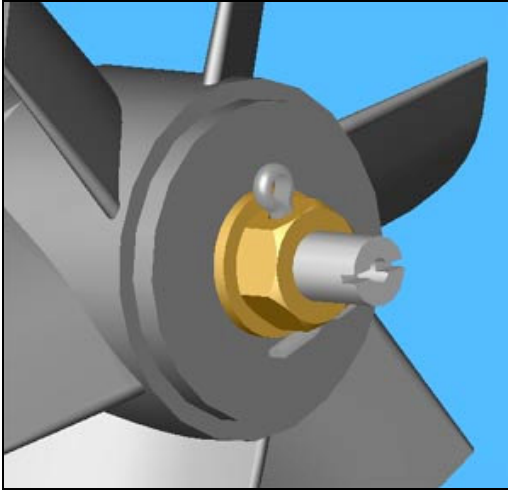


Figure 10 : Split Pin Retaining Fan

The modification of the attachment of the fan to the adaptor was more straightforward. A hole was drilled through the nut holding the fan and the adaptor. A split pin was then fitted through this hole.

Analytical Ducted Fan Optimisation

The previous design of flying platform utilised five identical electric motor driven ducted fans powered by a remote battery pack via an umbilical chord. At the current stage of development an attempt has been made to remove the umbilical chord. It was decided that this could be achieved by generating a larger proportion of lift from a larger central duct unit, this unit being powered by an internal combustion (IC) engine via direct mechanical drive.

During the development of the flying platform it started to become apparent in late 2003 that commercially available ducted fan units were either of inappropriate size or not sufficiently lightweight. A unit has currently been purchased but it has been estimated that it will provide insufficient lift to enable the carrying of a payload. Initial analysis has indicated that a substantially larger ducted fan would enable greater lift for the same power input while remaining dimensionally compatible with the platform structure. This could enable the platform to carry the specified payload.

The general trend for larger fans to give a better lift to power input ratio is illustrated by considering a number of known designs. Table 1 and Figure 11 show that there is a strong correlation between rotor size and lift to power ratio, with the power required reducing as rotor size increases. This appears to confirm that an increased fan diameter will increase the payload of the platform.

Table 1¹⁶ : Data on Known Static Thrust Generating Devices

VTOL Aircraft	Rotor Radius (r)	Rotor Type	Max. Takeoff weight	Takeoff Thrust (T)	Max. Power at Takeoff	Lift to Power ratio	$\frac{r^2}{T}$
	(m)		(kg)	(kN)	(kW)	(N/kW)	(m^2/N)
CH-47	9.3	Twin Rotor	22,680	222	2,339	95.1	97
EH-101	9.3	Single Rotor	16,450	161	14,782	91.6	134
Cypher	0.61	2x contra-rotating	136	1	34	39.2	70
Control fans	0.045	Ducted Fan	1.01	0.01	0.408	24.3	51
Ramtec	0.0665	Ducted Fan	3.75	0.0368	2.796	13.2	30

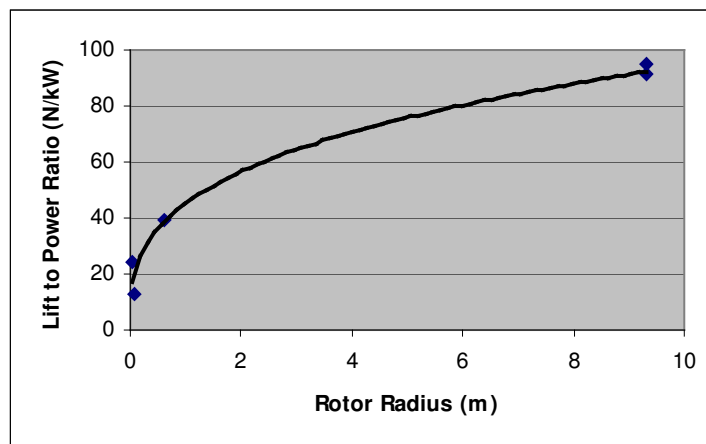


Figure 11 : Correlation between Rotor Radius and Lift Efficiency

A ducted fan is a thrust generator consisting of an axial flow impeller enclosed within an open tube or ‘duct’. As the blades move interaction with the air causes a continuous mass flow of air to accelerate up to some velocity causing an equal and opposite force on the blades. The performance of a ducted fan is closely related to the performance of the impeller within it. This study concentrates on the design of the impeller, further work concerning the duct has been carried out by other members of the group.

Traditionally there have been two methods of predicting the performance of axial flow impellers using analytical techniques and more recently an alternative technique has been published. This study details all three methods with special reference to the ducted fan required for an innovative autonomous flying platform being developed at The University of Exeter.

The simplest method is the *Blade Element* theory, which uses aerofoil theory to integrate over blade lengths to determine the total static thrust developed directly. Although simple to implement the assumptions made mean that this method is likely to be inaccurate for the case of a ducted fan. The other traditional method involves considering changes in velocity and applying *Bernoulli's* equation to determine differences in pressure and energy, this approach involves *Euler's* equation. This has also been shown to give inaccurate results when compared with experimental data.

A more recent approach considers the displacement of fluid by the blades and gives a very good correlation with experimental data. This method enables the type of general lift estimation required to design the major dimensions of the fan. Adjusting blade inlet and outlet angles using Euler's equation can then refine the design. Further work will be required to apply the displacement theory to the optimisation of the fan unit.

Blade Element Theory

It is logical to begin with the simplest analysis. Although this approach assumes infinitely long blades, parallel airflow across the aerofoil sections and takes no account of losses it can still give some understanding of how performance will be affected by changing the fan geometry.

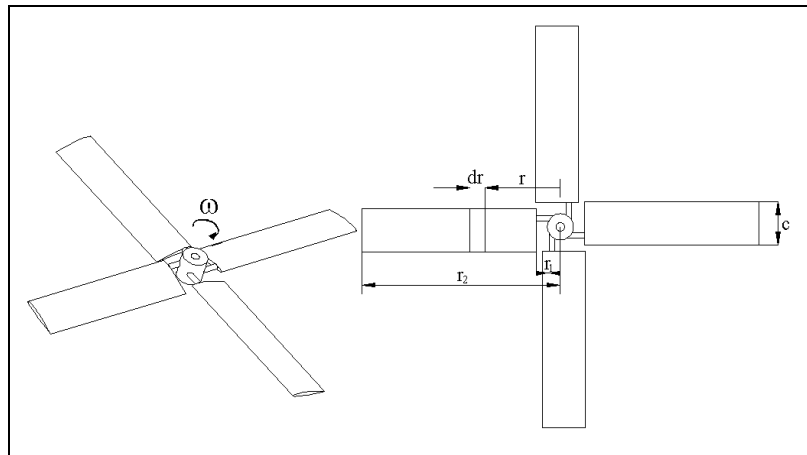


Figure 12 : Blade Element

Theory

Consider the simple four bladed propeller shown in Figure 12 rotating about its axis with rotational velocity ω

According to aerofoil theory¹⁷ a blade gives lift F_L given by Equation 1.

$$F_L = \frac{1}{2} \rho \cdot u^2 A \cdot C_L$$

Equation 1

where ρ is the density of air, A is the area of the wing (chord multiplied by span), and C_L is the coefficient of lift as determined for the specific aerofoil.

u is the velocity of the aerofoil relative to the air, this is a function of r and is given by

$$u = a \cdot r \quad \text{Equation 2}$$

To find the total lift given by a blade it is therefore necessary to consider a small strip of blade at radius r and of thickness dr and integrate over the length of the blade.

$$F_L = \int_{r_1}^{r_2} \frac{1}{2} \rho \cdot \omega^2 r^2 c \cdot C_L dr$$

where c is the chord of the blade.

Completing the integration and multiplying by the number of blades (N) gives the total lift

$$F_{L_{Tot}} = N \cdot \frac{1}{6} \rho \cdot \omega^2 c \cdot C_L \cdot (r_2^3 - r_1^3) \quad \text{Equation 3}$$

Similarly the drag force acting on each small length of blade is given by

$$\delta F_D \approx \frac{1}{2} \rho \cdot (\omega \cdot r)^2 c \cdot \delta r \cdot C_D$$

While the total power required is given by

$$\delta W_D \approx a \cdot r \cdot \delta F_D$$

Integrating over the length and multiplying by the number of blades gives the total power consumed.

$$W_{tot} = N \cdot \frac{1}{8} \rho \cdot \omega^3 c \cdot C_D \cdot (r_2^4 - r_1^4) \quad \text{Equation 4}$$

Rearranging Equation 4 in terms of ω and inserting into Equation 3

$$F_{L_{Tot}} = N \cdot \frac{1}{6} \rho \cdot \left(\frac{8 \cdot W_{tot}}{N \cdot \rho \cdot c \cdot C_D \cdot (r_2^4 - r_1^4)} \right)^{\frac{2}{3}} c \cdot C_L \cdot (r_2^3 - r_1^3) \quad \text{Equation 5}$$

Using Equation 5 it is possible to determine the lift generated by a given propeller for a given power input. This makes it possible to examine the performance of different fans with a constant power input.

Replacing all constant terms with the single constant a .

$$F_{L_{Tot}} = \left(\frac{1}{r_2^4} \right)^{\frac{2}{3}} \cdot r_2^3 = \frac{r_2^3}{r_2^{\frac{8}{3}}}$$

where a is a constant, this simplifies to

$$F_{L_{Tot}} = a \cdot r_2^{\frac{1}{3}} \quad \text{Equation 6}$$

Empirical data should be fitted to a curve of this form.

Comparison with Test Results

Using test data for the control fans it is possible to check the accuracy of this method. The power input, number of blades, average chord, hub radius and rotor radius were all input directly from the actual fan geometry and test conditions. The coefficient of drag was then adjusted to give the rotational velocity observed during testing. From this an appropriate coefficient of lift was also found from the simple assumption that the coefficient of lift will be approximately an order of magnitude greater than the coefficient of drag.

Applying Equation 5 it was found that the this theory calculated the lift to be approximately 5 times greater than was found during testing. The values used for the coefficients of lift and drag were also well outside the normal range for airfoils. It was therefore decided to attempt to correct the theoretical calculation by adjusting these coefficients. By setting C_d equal to **0.69** and C_L equal to **1.3** the theoretical equations produced results similar to those found experimentally. This appears a reasonable initial approach since the coefficient of lift is within the normal range while the coefficient of drag is considerably higher than would be normal for a simple aerofoil; explained by the much greater losses in such a system where there are very high interference and tip losses.

The large disparity of the coefficients required to give realistic results when compared to expected values for the coefficients is a cause for concern however. More detailed analysis is required to predict with any degree of certainty the actual performance of a given fan geometry before further development can take place.

Determining Optimum Fan Design

A spreadsheet was constructed to calculate total lift (Equation 5) and the speed at the blade tips, this was checked by manual calculation. The constant values are given in Table 2.

Table 2

Density of Air ¹⁸	1.2 kg/m ³
Power input	1000 W
Number of Blades	4
Chord	0.071 m
Coefficient of Lift	1.6
Coefficient of Drag	0.16
Hub Radius	0.05 m

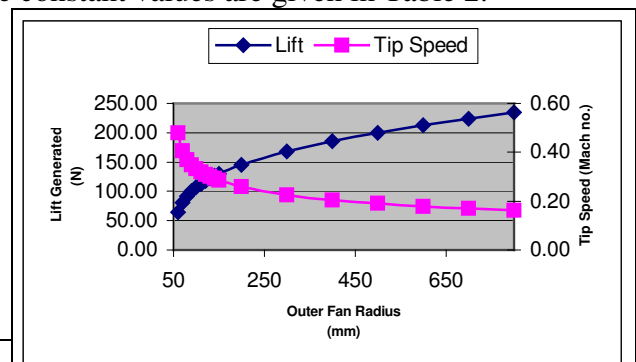


Figure 13 : Effect of increased Diameter

Figure 13 shows that the lift available is higher for any given power input if the outer fan diameter is increased, this is clear from Equation 6. It can also be seen that increasing the radius has the beneficial effect of reducing the tip speed.

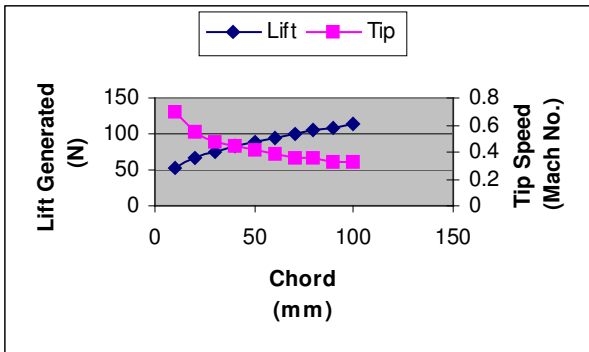


Figure 14 : Effect of increased Chord

Increasing the chord also increases the lift and reduces the tip speed within a practical range. Lift is increased despite the fact that increasing the chord also increases the inner radius and so reduces the total area giving lift.

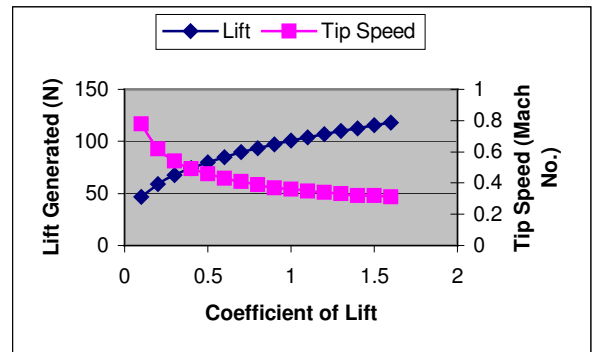


Figure 15 : Effect of increased Lift Coefficient

The coefficient of lift can be increased to around 1.6 by increasing the angle of attack. This creates a corresponding increase in the coefficient of drag but since this term is raised to a lower power the overall effect is an increase in lift.

The number of blades has relatively little effect on lift. A smaller number would simplify manufacture. The thrust produced by two blades is around 90% of the thrust of a four-blade fan, while a three-blade design gives over 95% of the thrust for an equivalent six blade design.

The analysis indicates that large increases in static thrust produced for a given power input are likely by increasing the fan diameter. This could substantially increase the performance of the flying platform.

However, these figures cannot be regarded as reliable due to assumptions made. Particularly the assumption that airflow will be parallel over the aerofoil section is not valid since the blades have a very low aspect ratio and so the air will travel in a noticeable arc, especially near the hub.

More complex analysis of this type may take into account some losses^{19,20} but this remains a relatively inaccurate approach.

Momentum Theory

Consider the flow of air through an annulus of the fan in the plane perpendicular to the flow of air as shown in Figure 16. Assuming that there is no flow in the radial direction the flow within the annulus can be ‘unrolled’ to represent the flow through the ‘cascade’ of blades as shown in Figure 17. This assumes that there are an infinite number of blades continuously acting on the flow. If the fan is rotating at an angular velocity ω then the blades will move through the control volume at a velocity $u = \omega \cdot r$

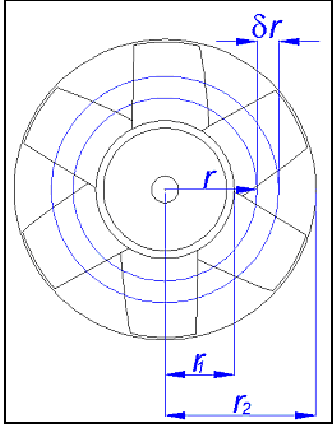


Figure 16 : Fan Annulus

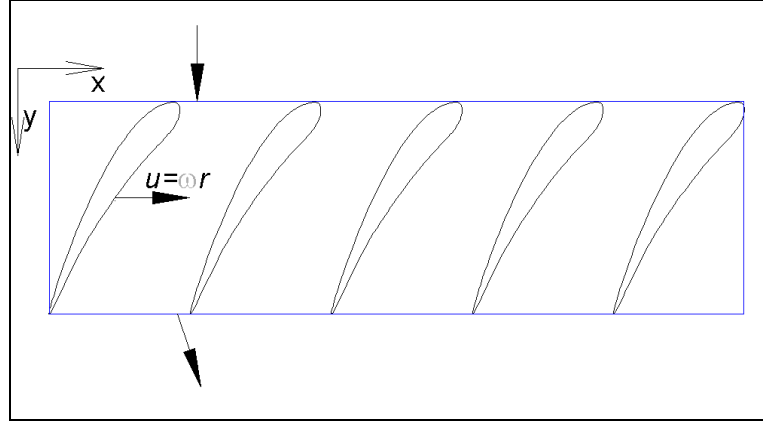


Figure 17 : Annulus ‘Unrolled’

Also shown in Figure 17 is the direction of the flow into and out of the control volume. Assuming that the tangential velocity is zero as it enters the fan axially, it will have some tangential velocity imparted on it by the movement of the blades.

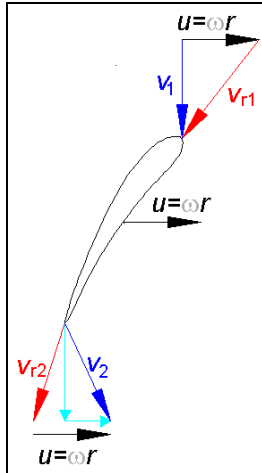


Figure 18 : Inlet and Outlet Triangles

Examining the components of velocity on either side of the control volume it is possible to determine the forces exerted on the cascade of blades²¹. The various velocities are shown in Figure 18, those in blue represent the absolute flow velocity, the absolute velocity of the blades is shown in black and the velocities of the flow relative to the blade are shown in red.

To simplify the analysis initially we can assume that the velocities do not vary with r , this assumption is reasonable if we imagine the average flow at a radius equidistant from r_1 and r_2 . Since all mechanical power (E) is delivered rotationally the momentum equation can be applied²² to show that, assuming no losses

$$E = \dot{m} \cdot (v_{x2} - v_{x1})$$

where \dot{m} is the mass flow rate and v_{x1} and v_{x2} are the initial and final components of velocity in the x direction.

Applying Euler’s Equation for energy per unit mass on either side of the control volume

$$\frac{P_1}{\rho} + \frac{v_1^2}{2} + E = \frac{P_2}{\rho} + \frac{v_2^2}{2}$$

Rearranging to give the pressure difference and multiplying by the area gives the total lifting force (F_L)

$$F_L = \pi \cdot (r_2^2 - r_1^2) \cdot \rho \cdot \left(E - \frac{v_{x2}^2}{2} \right)$$

This indicates that lift can be increased by; increasing the surface area of the fan, increasing the energy input or increasing the amount of tangential velocity imparted on the flow. The tangential velocity can be shown to be a product of the angle of the blade outlet tip β by applying trigonometry to Figure 18.

$$v_{x2} = \omega \cdot r - \frac{v_1}{\tan \beta}$$

This approach clearly implies that the outlet tip angle is the most important design consideration and that the blade chord has no effect on lift generated. This is in direct conflict with the aerofoil theory presented in the last section. The major assumption made by this analysis is that the blades are arranged so that the airflow is tangential to the blades from the leading to the trailing edges. In practice a blade of a given size and shape can only interact effectively with a limited flow rate of fluid and so this assumption is often not valid. It has been shown that this approach often gives results that differ substantially from experimental data.²³

Momentum theory is often used to determine blade angles but is clearly inadequate for estimations of the lift obtainable from different sizes of fan. Once general design dimensions and operating parameters have been defined by some other method this theory becomes useful to refine blade angles using the more standard approach described in the references.

Displacement Theory

It can be seen from Figure 19 that as the blades move they will displace a volumetric flow of the fluid equal to

$$\delta Q_x = (U - v_x) \cdot c \cdot \sin \beta \cdot \delta r$$

Equation 7

By rearranging the aerofoil equation and substituting for the components of relative velocity it can be shown that the lift is proportional to the displaced volume²⁴. This contradicts the assumption of the momentum theory that the chord has no affect on lift.

Although simple, Equation 7 is difficult to implement since the tangential component of the fluid's velocity (v_x) changes as the flow moves through the impeller. Therefore before integrating an annulus over the area of the impeller it is first necessary to integrate over the length of the blade in the y direction to find the affect that the blade has on the flow, see Figure 20.

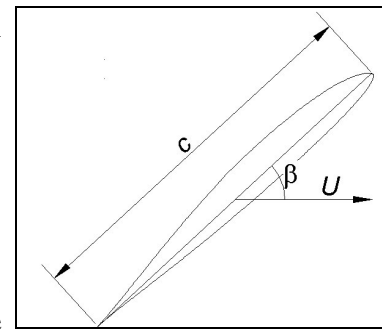


Figure 19 : Aerofoil Angle of Attack

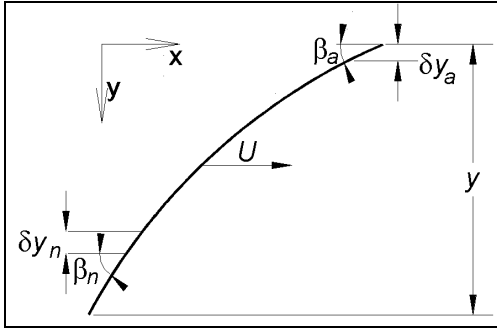


Figure 20 : Aerofoil Simplified to a Plate

Replacing the $c \cdot \sin \beta$ term in Equation 7 with the new term Y gives

$$\delta Q_x = (U - v_x) \cdot Y \cdot \delta r$$

This volume has been directly acted on by the blade and so must follow its contour, it therefore leaves distance δY_a with a component of velocity in the x direction of

$$v_{xa} = U - \frac{v_y}{\tan \beta_a}$$

The amount of fluid passing between two blades (δQ_I) will be greater than the fluid acted upon by the small strip δY and so the fluid that has been accelerated by interaction with the blade will interact with the rest of the flow and an uneven distribution of velocity will result. The exact manner of this interaction is not known but considering the momentum added to the volumetric flow δQ_x it is possible to say that the power added to the volumetric flow δQ_I will be

$$\delta E_a = \rho \cdot \delta Q_{xa} \cdot U \cdot v_{xa}$$

where δE_a is the power added to the volumetric flow passing between two blades over the distance δY_a .

The solution up to this point is adapted directly from the referenced papers published by S. Yedidiah but the application of the theory beyond this is not explained in the literature. In order to apply the theory it is necessary to substitute for terms that vary with Y and with r , and complete integrations for both of these variables. It is not yet clear whether this can be treated as a double integral. This will give the changes in energy and velocity. If Euler's equation is applied, in the same way as in the previous section, before integrating then the total lift force can be found.

At this stage it appears that the analysis will involve the following stages

1. Substitute functions of r and Y into the equation for changes in velocity over a thin layer of an annulus. This is derived from the displacement theory proposed by S. Yedidiah.
2. Apply Euler's equation to convert the previous equation into the pressure difference.
3. Multiply by the area of the annulus to get the force
4. Integrate over both r and Y to find the total lift force.

Adapting the theory in this way proved difficult. The displacement theory appears to provide the necessary analytical tools to specify the major parameters for the ducted fan unit such as the diameter, chord and number of blades. The accuracy of this approach has been shown to be high when compared with experimental data with predicted values within 20% and often significantly closer.²⁵ However, applying this theory to the optimisation process was not feasible within the time constraints of the project.

Design Approximations

None of the analytical methods were suitable for specifying the major design parameters such as overall diameter and chord. It was therefore necessary to estimate sensible values based on existing fan designs, the data in Table 1 was used. The performance indicator of primary importance is the lift to power ratio, this was therefore plotted against different quantities looking for correlations.

Figure 21 shows a strong correlation between two ratios; the ratio of rotor diameter over thrust and the ratio of lift over power. This shows that an aircraft of a given mass will require exponentially less power to lift it as the size of its rotor is increased.

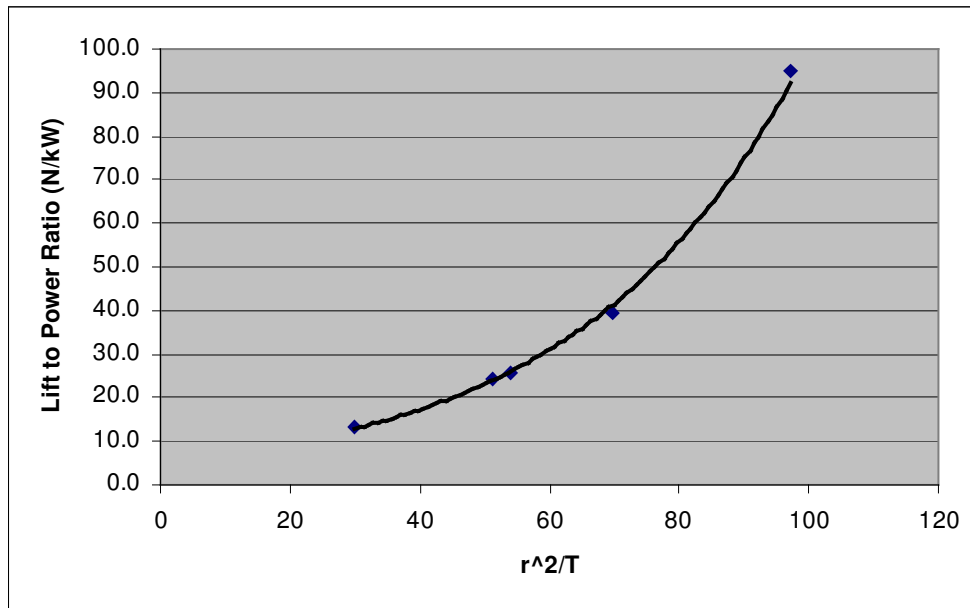


Figure 21 : Relationship between r^2/T and Lift Efficiency

Alternatively this correlation can be used to estimate the static thrust available from fans of different sizes with a constant power input. The process of obtaining these results is iterative; finding the value for static thrust that best fits the data. The data thus plotted showed a linear relationship between increasing fan radius and increasing static thrust.

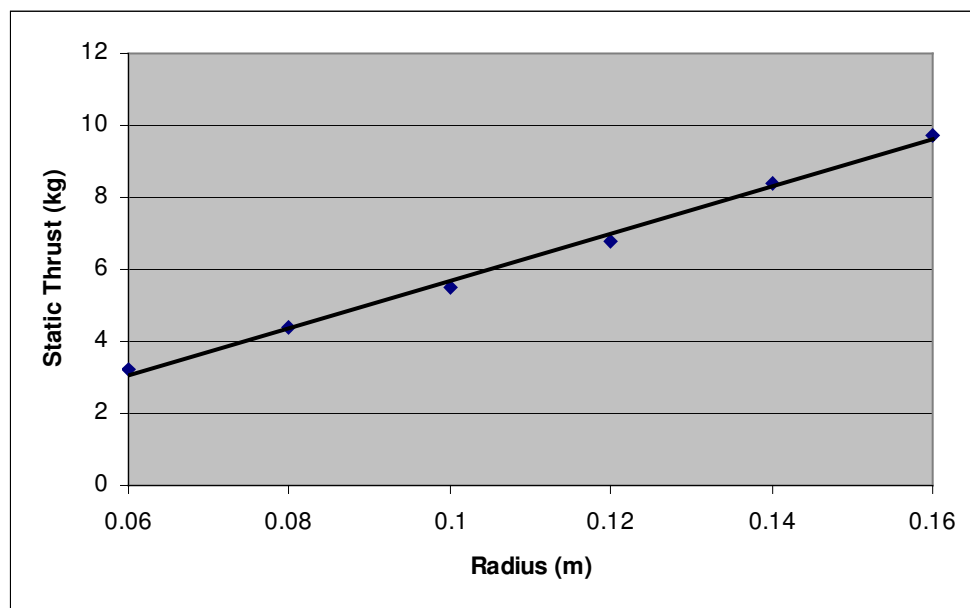


Figure 22 : Increase in Lift for Fixed Power with increasing Radius

If an *OS 1.4 RX-F1* is used then the input power is 2.6 kW at 9000 rpm and the engine will be 260 g heavier than the current engine. Based on initial modelling of fan geometry the fan weight has been estimated for a single piece aluminium casting, this can be compared with the current fan centre at 160 g. Table 3 gives the estimated performance of different fan sizes using this engine.

Table 3 : Predicted Performance for larger Fan Sizes

Fan Radius (m)	Static Thrust (kg)	Fan Weight (kg)	Net Gain Static Thrust		Tip speed Mach no.
			(kg)	%	
0.1	5.5	0.36	1.3	34%	0.27
0.12	6.8	0.41	2.5	68%	0.32
0.14	8.4	0.65	3.9	104%	0.38
0.16	9.7	0.98	4.9	130%	0.43
0.18	11.5	1.39	6.3	167%	0.48
0.2	13.3	1.91	7.5	201%	0.54
0.22	15.2	2.54	8.8	235%	0.59

A radius of 120 mm was chosen as it was seen as a good compromise. It will increase static thrust sufficiently to ensure flight and allow some payload while remaining compatible with the current airframe layout. It also has the advantage of being small enough to allow rapid prototyping as a single piece.

There would be significant advantages in using a substantially larger fan. Although this would mean some changes to the layout of the airframe it would not require changing the overall size. A radius of at least 200 mm should be sufficient to allow a full 5 kg payload with a reasonable range. Unfortunately manufacture is likely to be extremely difficult at this size, gaining access to suitable rapid prototyping or 5-axis CNC machining facilities would likely be a major obstacle.

Conclusion to Fan Analysis

Both theoretical analysis and data on existing impellers shows that increasing fan diameter can enhance performance.

The aerofoil theory gives a useful insight into the important design parameters but is of no practical value in predicting actual performance since it is highly inaccurate for the type of geometry being considered.

Displacement theory provides the accuracy to specify the major parameters for the ducted fan unit such as the diameter, chord and number of blades. However, applying this theory to the optimisation process is relatively complex and further work will be required.

The momentum theory is useful in that it allows refinement of blade angles once the general design dimensions and operating parameters have been defined. Considerations of losses due to tip clearance²⁶ and suction reverse flow²⁷ can also be made at this point.

No consideration has been made in this study of the effects of the duct unit on overall performance. In order to produce a complete design the duct will also require study.

This report gives some insight into the different theories applied to ducted fan design and their practical value for the particular design problem faced by the Flying Platform group. However, there remain significant gaps in the understanding and considerable further work is required to produce an optimised fan design.

Fan Detail Design

The detail design as covered here begins with the basic specification as derived in the previous section. This is summarised in Table 4.

Table 4 : Fan Specification

Fan Radius	Static Thrust	Fan Weight	Net Gain Static Thrust		Tip speed
(m)	(kg)	(kg)	(kg)	%	Mach no.
0.12	6.8	0.41	2.5	68%	0.32

Calculation of Blade Angles

The inlet and outlet blade angles were calculated for no shock condition at 9,000 rpm. The standard approach using *Euler's* equation was applied.

Table 5 : 'Euler's' Spreadsheet

Design Points		
Outside Radius	(m)	0.12
Inside Radius	(m)	0.054
Pressure Difference	(Pa)	2717
Rotational Velocity	(rad/s)	942
Input Power	(W)	2500
Assumed Efficiency	(%)	80%
Fluid Density	(kg/m ³)	1.20

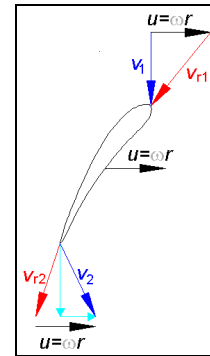
Directly Derived Variables		
Area	(m ²)	0.0361
Pressure Difference (<i>H</i>)	(m fluid)	230.80
Power output	(W)	2000
Flow rate	(m ³ /s)	0.736
Flow Velocity (<i>V_f</i>)	(m/s)	20.40

Blade Angle		1	2	3	4	5
Distance from Hub	(m)	0	0.0165	0.033	0.0495	0.066
Effective radius	(m)	0.054	0.0705	0.087	0.1035	0.12
Blade Velocity (<i>U</i>)	(m/s)	50.868	66.411	81.954	97.497	113.04
Inlet Angle (<i>β₁</i>)	(deg)	21.9	17.1	14.0	11.8	10.2
Outlet Angle (<i>β₂</i>)	(deg)	72.7	32.3	20.6	15.4	12.4
Whirl Velocity (<i>V_w</i>)	(m/s)	44.51	34.09	27.63	23.22	20.03

Table 5 shows the spreadsheet used to calculate the inlet and outlet tip angles for the fan blades at different radiuses. The equations are derived from the inlet and outlet triangles and *Euler's* equation.

$$\beta_1 = \tan^{-1}\left(\frac{V_f}{U}\right)$$

$$\beta_2 = \tan^{-1}\left(\frac{V_f}{U - \frac{H \cdot g}{U}}\right)$$



This spreadsheet is available for use by future students. The angles for any fan may be calculated at any five sections by adjusting the relevant parameters.

Initial Stress Analysis

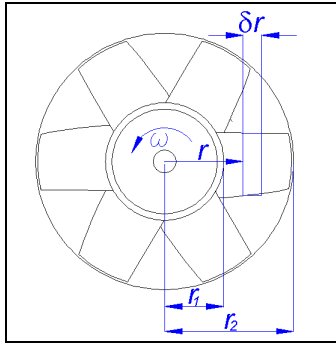


Figure 23

A simple stress analysis was completed before further detailed design work took place.

The force acting on the root of the blade due to centripetal acceleration acting on a small strip of thickness δr is given by

$$\delta F = r \cdot \omega^2 \cdot A \cdot \delta r \cdot \rho$$

Integrating between r_1 and r_2 gives the total force on the root of the blade.

Assuming the blade area does not vary with r then dividing through by the area gives the stress on the root.

$$\sigma_{root} = \frac{1}{2} \rho \cdot \omega^2 (r_2^2 - r_1^2)$$

Taking the material properties of aluminium alloy²⁸ 6061-T6 as a density of 2,700 kg/m³ and yield stress of 270 M Pa. With an angular velocity of 942 rad/s the stress on the blade root due to centripetal acceleration will be 13.8 M Pa. This is approximately 20 times the yield stress of 6061-T6 aluminium alloy. This makes the design seem quite feasible and indicates that it will not be necessary to taper the blades in order to achieve the required strength.

The use of a directly rapid prototyped fan produced using the stereolithography process was also considered. This was found to be inappropriate for two reasons. Firstly the resin is toxic leading to greater dangers should the fan burst. Secondly even the strongest polymers used in this process are only marginally strong enough.

3D CAD Modelling

Detailed aerofoil coordinate data for the sd6060 profile was entered into AutoCAD, this was then scaled, simplified and modified. The number of points was reduced to 16 and a radius was added to the trailing edge for manufacturing purposes. The point data is given in Figure 24.

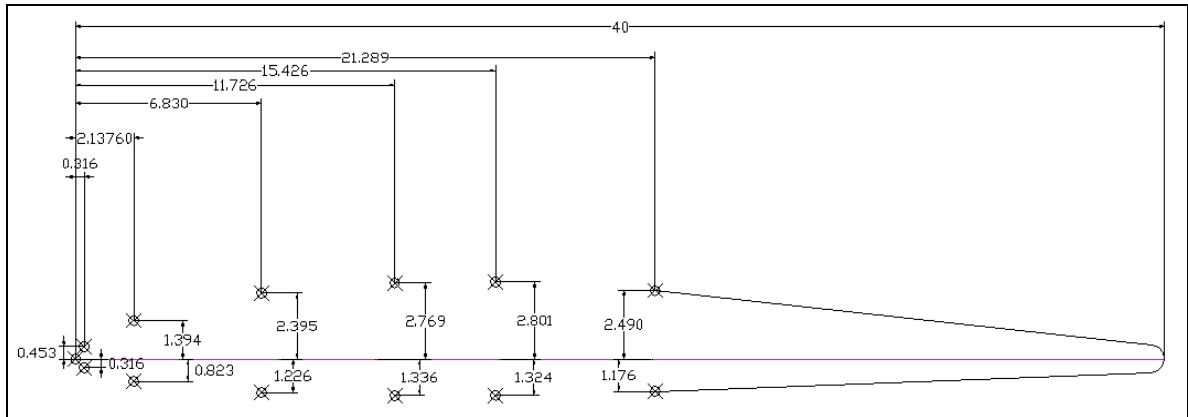


Figure 24 : Aerofoil Section Point Data

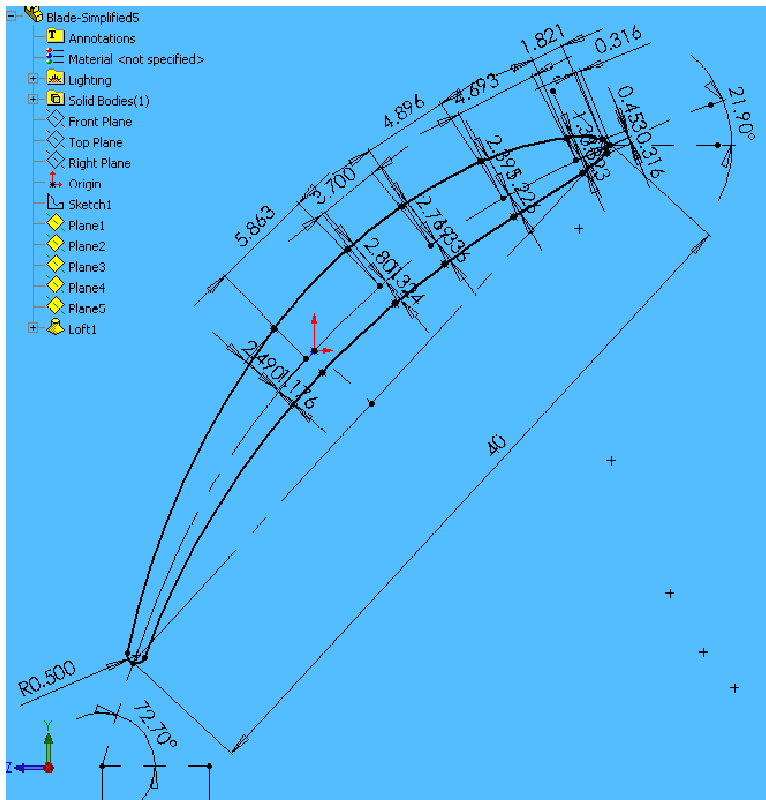


Figure 25 : Sketch in Parametric Model

All of this standard point data was represented as the distance from the centre line. This enabled the data to be dimensioned from a radiused centre line (measured on the normal to the curve) within the Solidworks CAD package. This curved center line was then aligned in such a way that the inlet and outlet angles could be adjusted as parameters.

This approach enabled a highly accurate geometry to be constructed in CAD with relative ease. The model will be available for future students to use. It allows a fan of any geometry to be created easily by simply adjusting parameters.

The detailed manufacturing design was completed at this stage since from this point it was relatively straightforward. This then allowed assessment of manufacturing feasibility.

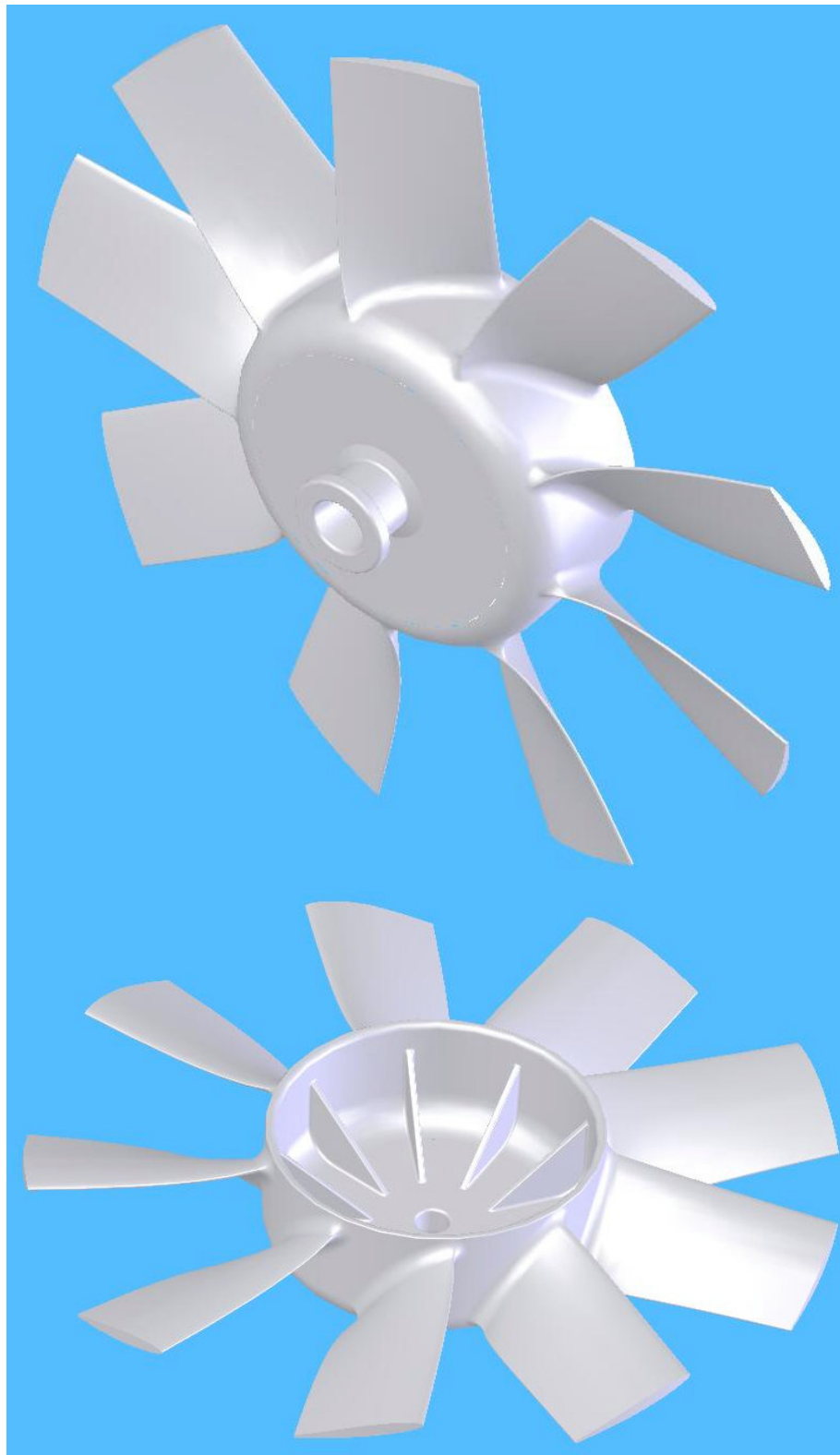


Figure 26 : Fan Design suitable for Investment Casting

The geometry was simplified considerably before exporting for computational fluid dynamics (CFD) analysis. This was achieved by modelling the nose cone as part of the main fan body and removing all internal detail. The majority of fillets were also removed. The model was then cut away at 40° to leave a single blade.

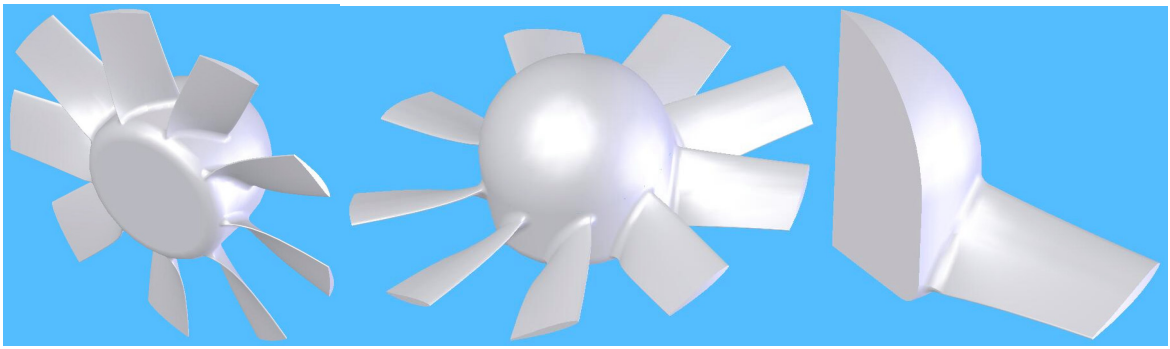


Figure 27 : Fan Design Simplified for CFD Modelling

The raw point data (110 3D points) was then exported and used as the basis for modelling in *Gambit*. The geometry was further simplified within *Gambit* to 72 points and the volume was divided into a number of layers to allow mesh refinement around the fan blade and a much coarser mesh some distance away. This allowed efficient meshing ready for analysis using the CFD code *Fluent*.

Tet hybrid elements were used with a TGrid meshing scheme. The mesh was checked for equiangle scwness and appeared to be of a high quality.

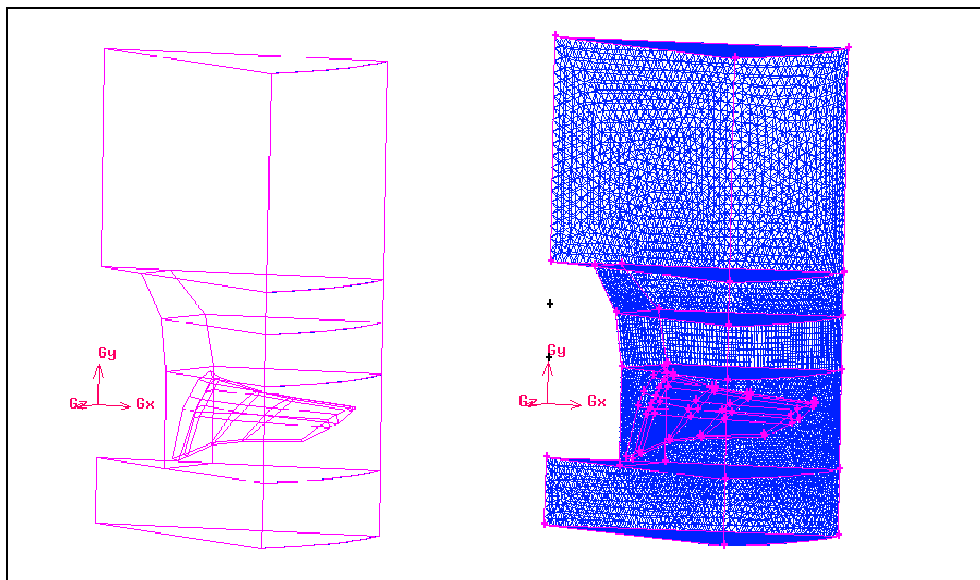


Figure 28 : Final Geometry before and after Meshing

Computational Fluid Dynamics (CFD) Analysis

Boundary Conditions and Set-up

Details of geometry creation and meshing are covered in the previous section.

Use of ‘periodic’ boundaries was central to the modelling strategy. This allows the segment of the complete fan to be modelled as though it were a part of the whole fan. Any changes in flow caused by the blade in one direction are felt by the blade from the other direction. This boundary condition involves specifying two planes on opposite sides of the modelled region, flow out of one face flows into the opposite face. This creates a rotational symmetry; in this case nine degrees of rotational symmetry with pairs of faces at 40 degrees to one another.

A velocity inlet and a pressure outlet were used with the remaining faces set as walls. The velocity inlet was used to specify both the flow velocity and the rotational velocity of the

fan since in this model it is the fan that is the fixed reference frame with the air moving not just through but also around it. The outer radius of the region was set as a wall with an angular velocity equal to that of the inlet air, this simulates the fixed duct present in the actual fan.

Results

The model was solved using both k-epsilon and Reynolds stress turbulence models. It was converged with residues of less than 10^{-4} .

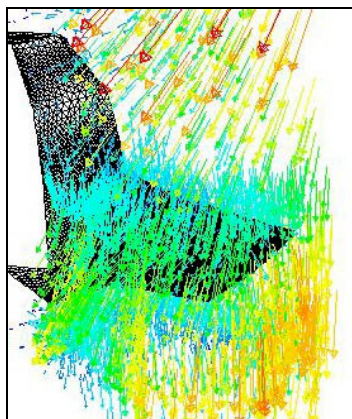


Figure 29 : CFD Results

Visual results were obtained which appeared sensible.

Forces in the axial direction on all the faces of the fan were totalled and multiplied by the number of blades to give the lift force. The boundary regions were also grouped according to distance from the centre. The force on each group in the tangential direction was multiplied by the average distance from the axis to give the moment. The moments were totalled, multiplied by the number of blades and then by the angular velocity, this gave the power consumed.

This showed that the fan would be expected to consume 3.05 kW while producing 13.3 kg static thrust.

Conclusion

General analysis of the fan design has been highly successful. A sound design has been identified that is expected to provide a substantial performance increase.

A strategy for more detailed refinement and performance verification using CFD has also been identified. Unfortunately due to time constraints and unforeseen problems at all stages of this work the final CFD analysis is inconclusive. However, work is ongoing and conclusive results are expected for the final presentation on this work.

Fan Manufacture

No manufacture has currently taken place. However, the fan has been designed in consultation with *Howmet Castings* who are able to produce a rapid prototyped pattern suitable for use in investment casting. They are not able to cast the fans as they only cast in highly dense super alloys at Exeter. However *Aeromet* are able to cast the completed fan.

Conclusion

Work concerning the ducted fan units has been largely successful. The four existing units have been found to be suitable for control purposes with the modifications carried out. Work on the larger central unit has been successful in identifying the potential increase in performance. A suitable detailed design and manufacturing route have also been identified. However, due to time constraints manufacture has not been completed.

CFD work has partially proven the performance of the suggested unit. However, it would be advised that some further work be carried out before manufacture if this is possible within the time constraints. The manufacturing geometry has been input to the CAD system as a parametric model. In addition a spreadsheet has been created allowing very rapid calculation of blade inlet and outlet angles. This will allow future students to alter the design with a minimum of work if this is found to be beneficial.

Manufacturing contacts at *Howmet Castings* are aware that the project is ongoing and are prepared to work with students in 2004-5.

References

- ¹ Whitaker B., 'Western deaths spark Middle East terror alert', The Manchester Guardian, Wednesday March 19, 2003
- ² Hambling D., 'The war after next', The Manchester Guardian, Thursday January 23, 2003
- ³ Withington T., 'America's forces patrol the world', The Observer, Sunday April 6, 2003
- ⁴ Henley J., 'Eyes in the sky to guard G8', The Manchester Guardian, Tuesday May 27, 2003
- ⁵ Adam D., 'Is it a bird? Is it a plane?', The Manchester Guardian, Thursday June 12, 2003
- ⁶ Mullens K.D. et al, 'An Automated UAV Mission System', SPAWAR Systems Center
- ⁷ Murphy D.W., Bott W.D., Bryan J.L., Coleman D.W., Gage, H.G., 'MSSMP: No Place to Hide', United States Army Military Police School
- ⁸ Rotorhub, "Fire Scout Officially Joins US Army", 29th January 2004,
- ⁹ <http://www.spawar.navy.mil/robots/images/cypher3.jpg>
- ¹⁰ Murphy D., Cycon J., 'Applications for mini VTOL UAV for Law Enforcement', Space and Naval Warfare Systems Center.
- ¹¹ Murphy D.W., et al, "Air-Mobile Ground Surveillance and Security System (AMGSSS) Project Summary Report", Defence Special Weapons Agency and the Physical Security Equipment Management Office of the Army Aviation and Troop Command, September 1996
- ¹² http://avia.russian.ee/vertigo/foto/sik_cypher2.jpg
- ¹³ Kondor, S., Heiges, M. "Active Pneumatic Flow Control for Control of A Ducted Fan", AIAA Paper 2001-0117, Jan 2001
- ¹⁴ Defence Systems Daily, 'BAe Systems and QinetiQ to collaborate on ISTAR and UAV's', 12th September 2001.
- ¹⁵ Newport News, VA, 'Allied Aerospace VTOL UAV attains full-autonomy', April, 2004
- ¹⁶ Murphy, D., W. et al, "Air-Mobile Ground Surveillance and Security System (AMGSSS) Project Summary Report", Defence Special Weapons Agency and the Physical Security Equipment Management Office of the Army Aviation and Troop Command, September 1996
- ¹⁷ Douglas J.F., Gasiorek J.M. and Swaffield J.A.; 'Fluid Mechanics', 3rd Edition, 1995, Longman, pg 374-375
- ¹⁸ Rogers G.F.C. and Mayhew Y.R.; 'Thermodynamic and Transport Properties of Fluids; SI Units', 5th Edition, 1995, Blackwell Oxford UK and Cambridge USA, pg 16
- ¹⁹ Douglas J.F., Gasiorek J.M. and Swaffield J.A.; 'Fluid Mechanics', 3rd Edition, 1995, Longman, pg 380-385
- ²⁰ Glauert H; 'The Elements of Aerofoil and Airscrew Theory', 2nd Edition, 1947, Cambridge Science Classics, pg 208-221
- ²¹ Foa J.V., 'Elements of Flight Propulsion', 1960, John Wiley & Sons, pg 202-210
- ²² Horlock J.H.; 'Axial Flow Compressors', 1958, Butterworths Scientific Publications, 29-38
- ²³ Yedidiah S, 'An Overview of Methods for Calculating the Head of a Rotodynamic Impeller and their Practical Significance', Proceedings of the Institute of Mechanical Engineers, 24th February 2003 Vol. 217 Part E
- ²⁴ Yedidiah S; 'Present Knowledge of the Effects of the Impeller Geometry on the Developed Dead', Proceedings of the Institution of Mechanical Engineers Part A-Journal of Power and Energy, 1996
- ²⁵ Yedidiah S, 'An Overview of Methods for Calculating the Head of a Rotodynamic Impeller and their Practical Significance', Proceedings of the Institute of Mechanical Engineers, 24th February 2003 Vol. 217 Part E
- ²⁶ Senoo Y, 'Mechanics on the Tip Clearance Loss of Impeller Blades', Journal of Turbomachinery – Transactions of the ASME, October 1991.
- ²⁷ Alpan K & Peng WW, 'Suction Reverse Flow in an Axial-Flow Pump', Journal of Fluids Engineering – Transactions of the ASME, March 1991
- ²⁸ Gere and Timoshenko, 'Mechanics of Materials', Third SI Edition, 1991, Chapman and Hall, pg 778-780